Vol. 46, No. 4 (2024) 709-721, DOI: 10.24874/ti.1760.09.24.11

Tribology in Industry

www.tribology.rs

RESEARCH

Influence of Bias Voltage on the Microstructure, Mechanical and Corrosion Properties of Ti/CrN/TiN Multilayered Films Deposited by Cathodic Arc Evaporation

Vu Van Huy[a,*], Nikolay B. Rodionov[b], Valery A. Karpov[c], Ngo Thanh Binh[a], Nguyen Dang Khoa[d], Vu Thi Lan Vi[d]

[a]*Joint Vietnam-Russia Tropical Science and Technology Research Center, Vietnam,*
[b]*Troitsk Institute of Innovative and Thermonuclear Research, Russia,*
[c]*Institute of ecology and evolution A.N. Severtsov of the Russian Academy of Sciences, Russia,*
[d]*Ho Chi Minh City University of Technology (HCMUT), Vietnam.*

Keywords:

PVD
Corrosion behavior
Ti/CrN/TiN coating
Multilayer film
Bias
Macroparticle

* Corresponding author:

Vu Van Huy
E-mail: huy241989@gmail.com

Received: 24 September 2024
Revised: 25 October 2024
Accepted: 15 November 2024

A B S T R A C T

Ti/CrN/TiN multilayer coatings were deposited via cathodic arc deposition at substrate bias voltages ranging from 20 V to 60 V. The study investigated the effects of bias voltage on the coatings microstructure, mechanical properties, and corrosion properties using laser and scanning electron microscopy, X-ray diffraction, nanohardness testing, and electrochemical testing equipment. The results indicate that bias voltage significantly influences the morphologies of Ti/CrN/TiN coatings. As the bias voltage increased from 20 V to 60 V, the concentration of macroscopic defects decreased markedly, and the average surface roughness (Ra) reduced from 0.227 μm to 0.179 μm. Nanoindentation revealed that coatings deposited at a bias voltage of 60 V exhibited a notable enhancement in hardness and elastic modulus. Corrosion testing in a 3.5 wt.% NaCl solution showed that coatings deposited at bias voltages of 20 V and 40 V had better corrosion resistance compared to those deposited at 60 V, likely due to the denser microstructure acting as a barrier to the diffusion of corrosive substances.

© 2024 Published by Faculty of Engineering

1. INTRODUCTION

Physical Vapor Deposition (PVD) is widely used in thin-film fabrication due to its ability to produce dense, high-purity films with excellent adhesion. Unlike Chemical Vapor Deposition (CVD), which relies on chemical reactions to deposit materials from gaseous precursors, PVD is a physical process, typically involving techniques such as sputtering or evaporation to transport target material atoms onto a substrate. While CVD methods, including Plasma-Enhanced CVD (PECVD), allow uniform coatings over large

areas and can be applied at lower temperatures (PECVD), they may result in impurity incorporation due to byproducts from chemical reactions. Transition metal nitride coatings deposited via physical vapor deposition (PVD) techniques serve as prominent materials for enhancing the surface properties of substrate materials, including corrosion resistance, hardness, wear-resistance, and machinability [1-5]. Consequently, they are well-suited for various applications in mechanical devices, cutting and forming tools, die casting molds, and plastic extrusion. It is widely acknowledged that the mechanical properties and corrosion resistance of deposited nitride films are significantly influenced by the specific deposition technique and processing conditions employed. Among the array of PVD variants, cathodic arc deposition stands out as one of the most utilized methods for depositing protective coatings, including CrN and TiN thin films. Distinguished by its generation of ions rather than neutrals or excited species, this technique yields highly charged states during deposition, facilitating the growth of high-quality films with superior density and adhesion properties. One drawback of this deposition method is the presence of a large number of macroparticles on the surface [6]. Macroparticles, which are generated by molten cathode material, can diminish coating adhesion, leading to increased roughness and porosity, or serve as abrasive particles within the coating. Furthermore, these defects may expedite substrate corrosion through the initiation of localized galvanic corrosion.

In order to mitigate the inconvenience caused by macroparticles, several plasma filtering techniques have been developed. However, achieving scalability for many filters proves challenging due to their geometry and the low deposition rate of coatings when using filters. Additionally, the impact of process parameters has been recognized as an effective approach to addressing this issue. Proper control of parameters such as cathode voltage, substrate temperature, gas ratio, and bias voltage enhances the performance of coatings and can reduce defect density. The bias voltage applied to the substrate influences the surface morphology as well as the mechanical and electrochemical properties of the films. A higher bias voltage can decrease the number and size of macroparticles, attributed to the increased momentum of the accelerated particles and the repulsive force resulting from alterations in the charging state of the macroparticles [7].

Talha Faizi et al. [8] conducted a comprehensive investigation into the influence of varying bias voltages on the hardness, elastic modulus, and corrosion resistance of TiN coatings deposited via magnetron sputtering onto stainless steel substrates. Their experimental setup involved bias voltage conditions of -50 V and -100 V. Their results revealed a notable reduction in surface roughness, decreasing from 2.7 nm (for the -50 V sample) to 1.8 nm (for the -100 V sample). This phenomenon was attributed to an etching-like process induced by ions with higher energies impacting the surface. Nanoindentation analyses indicated that the -100 V bias voltage yielded superior hardness and elastic modulus, attributable to its more compact packing and relatively less porous structure. Additionally, the authors observed that increasing bias voltage resulted in the formation of a densely packed, fine-grained columnar structure, thereby reducing the corrosion rate of the coatings.

However, several studies have indicated that the positive impact of bias on the structure and mechanical properties of coatings produced by the Physical Vapor Deposition (PVD) method is constrained. An excessive increase in bias may lead to detrimental effects on the mechanical and electrochemical properties of the films. For instance, Warcholinski et al. [9] investigated the variations in residual stress and hardness of CrCN and CrN films deposited via cathodic arc evaporation, altering the bias from -10V to -300V. Their findings revealed an initial increase in compressive residual stress and hardness with rising bias values; however, continued increments led to a subsequent decrease in compressive residual stresses and hardness. Specifically, maximum compressive residual stresses and hardness were attained at -70V and -150V, respectively. These results align with findings by Wang et al., [10] who explored the influence of negative substrate bias on the structure and properties of TiN

coatings fabricated via high-power impulse magnetron sputtering (HIPIMS). In the investigation of CrN coatings deposited by cathodic arc evaporation, M. Oden et al. [11] also observed similar outcomes. Specifically, they noted a reduction in compressive residual stress at elevated bias voltages. Nanoindentation analysis revealed a peak hardness of 29 GPa at a bias voltage of -100 V. The authors attributed these findings to lattice defect annihilation within the collision cascade and subsequent lattice defect diffusion during the deposition process.

The prevalence of microscopic defects exposing the substrate to corrosive media poses a significant challenge in physical vapor deposition (PVD) coatings. Extensive research has highlighted the detrimental effects of these defects. To address this issue, various strategies, including the use of multilayers, have been employed to mitigate the substrate-coating combination characteristic, thereby inhibiting defect formation [4].

Multilayer PVD coatings are engineered to enhance both the corrosion resistance and mechanical strength of surfaces, making them highly effective for applications in demanding environments. The primary function of these coatings is to improve surface durability by combining multiple thin layers of materials with complementary properties, often alternating between hard and ductile layers. This multilayer configuration is especially effective in blocking crack propagation, distributing mechanical stresses more evenly, and enhancing toughness. As a result, these coatings significantly improve mechanical properties such as hardness, elastic modulus, and resistance to wear and deformation.

Beyond mechanical performance, multilayer PVD coatings also play a critical role in enhancing corrosion resistance. The layered structure acts as a series of barriers that impede the penetration of corrosive agents, effectively reducing the rate of oxidation and chemical degradation of the underlying material. Each interface within the multilayer stack serves to limit the progression of corrosion pathways, thereby extending the lifespan of the coated component. By optimizing layer thickness, number of layers, and material selection, multilayer PVD coatings provide a high-performance solution with superior mechanical and corrosion-resistant properties, making them ideal for use in industries like aerospace, automotive, and heavy machinery [2,4].

Numerous research studies have emphasized the effectiveness of multilayered structures like Ti/TiN, Cr/CrN, and TiN/CrN in enhancing the corrosion resistance and mechanical properties of PVD coatings [1-4]. However, there is a gap in the study of the corrosion resistance and mechanical properties of Ti/CrN/TiN films deposited using the cathodic arc method at different biases. In this study, we investigated the impact of bias voltage on the surface roughness, electrochemical behavior, and mechanical properties of Ti/CrN/TiN multilayer coatings [2-5].

2. EXPERIMENT

Ti/CrN/TiN coatings were fabricated via cathodic arc evaporation utilizing the DSA 7504 PVD system. This system comprises a vacuum chamber with dimensions of Φ500 × 400 mm, accommodating two arc heads with target dimensions of Φ80 mm × 20 mm. Additionally, the setup incorporates one DC gun and one RF gun, each equipped with targets measuring Φ76.2 mm × 6.35 mm. The chamber underwent initial evacuation to achieve a base pressure below 9×10^{-6} Torr, followed by plasma etching through Ar glow discharge for 20 minutes. SS304 steel substrates sized at 50×50×1.5 mm underwent preparation involving polishing with 2000 sandpaper and subsequent finishing with 1 mm diamond paste. Preceding deposition, the substrates underwent ultrasonic cleaning in acetone and isopropanol, affixed onto a rotating sample holder at a distance of 20 cm from the arc target. The deposited coating comprises ten layers of Ti/CrN/TiN, with each layer composed of three sub-layers of Ti, CrN, and TiN, possessing thicknesses of 30 nm, 100 nm, and 100 nm, respectively. Thickness adjustment of each layer is achieved through modulation of coating time. Moreover, to enhance adhesion between the coating and substrate, an initial Ti interlayer

approximately 100 nm in thickness was deposited prior to the application of subsequent layers. The process parameters are illustrated in Table 1.

Table 1. Process parameters for Ti/CrN/TiN coatings deposition.

Sample	Temperature (°C)	Bias (V)	Rotation speed (rpm)	Arc2-Cr (A)	Arc1-Ti (A)	Ar (sccm)	N_2(TiN and CrN) (sccm)
M1	200	20	10	60	70	10	90
M2	200	40	10	60	70	10	90
M3	200	60	10	60	70	10	90

Surface morphology analysis of the coatings was conducted utilizing multiple microscopy techniques, including field emission scanning electron microscopy with the FE SEM S4800, laser scanning microscopy with the Laser Microscope OLS5100-SAF, and Inverted Microscopes Leica DMi8 M. ImageJ 1.53f software facilitated the quantification of macroparticle area on the coated sample surfaces, with calculations based on images acquired using the Leica DMi8 M microscope. Surface roughness assessment of the coated samples was performed employing the Portable Surface Roughness Measuring Instrument SURFTEST SJ-410 in conjunction with the Laser Microscope OLS5100-SAF. The latter utilizes a non-contact 3D method, scanning an area of 128 μm × 128 μm to derive the average roughness value.

The determination of coating thickness employed the calotest grinding method (CGM), whereby a hardened steel ball rotates freely against the coated sample surface until penetration occurs, with the penetration depth set at a minimum of twice the coating thickness. Utilizing measurements of the wear scar diameter in the circular projections of the coating, the thickness (t) of the coating was calculated using Equation (1) [12]:

$$t = \frac{D^2 - d^2}{8R} \quad (1)$$

where R represents the radius of the steel ball, D denotes the outer diameter, d indicates the inner diameter of the circular projections coating.

Phase structure analysis was conducted through X-ray diffraction utilizing a PANalytical Empyrean X machine equipped with CuKα radiation. The scanning speed (2θ/s) was maintained at 0.03º/s during the analysis. To evaluate film adhesion to the substrate, adherence tests were performed following the guidelines outlined in ISO 26443:2008 (E). These tests utilized a Rockwell hardness tester in conjunction with a Leica DMi8 microscope for comprehensive assessment.

The mechanical properties of the coatings underwent assessment via the nanoindentation technique employing the Nano Scan – 4D system. This method entails the measurement and analysis of the load's dependence on the penetration depth of the indenter upon application to the material surface. Mechanical testing utilized a Berkovich-type indenter, characterized by a trihedral diamond pyramid configuration with an apex angle approximately measuring 142º.

The polarization curve measurement in a 3.5% NaCl solution was conducted using the dynamic potential method employing an Autolab Metrohm PGSTAT302N device equipped with a three-electrode system. This system comprised a working electrode (WE) constructed from stainless steel coated with a Ti/CrN/TiN film, a reference electrode (RE) containing AgCl in Saturated KCl, and a counter electrode composed of platinum (Pt). The corrosion potential scanning range spanned from -1 V to 1 V, with a scanning rate set at 5 mV/s.

Prior to conducting the potentiodynamic polarization test, the samples were immersed in the solution for 300 seconds to establish the open-circuit potential. The corrosion potential (E_{corr}) and corrosion current (I_{corr}) were determined by Tafel polarization plot and modeling functions of the corrosion process in the Nova 2.1 software according to Equation (2) [13]:

$$i = i_{corr}\left[exp\left(\frac{2.303(E-E_{corr})}{b_a}\right) - exp\left(\frac{2.303(E-E_{corr})}{b_c}\right)\right] \quad (2)$$

where i is the current, i_{corr} is the current at corrosion potential E_{corr}, E is the applied potential, E_{corr} is the corrosion potential, b_a and b_c are Tafel constants which are anodic and cathodic slopes of *E-log I* plots in the Tafel regions.

Polarization resistance was determined using Equation (3) **Error! Reference source not found.**:

$$R_p = \frac{b_a b_c}{2.303(b_a b_c) i_{corr}} \quad (3)$$

3. RESULTS AND DISCUSSION

3.1 Microstructure and morphology

Fig. 1 displays the XRD patterns of Ti/CrN/TiN coatings at different bias voltages. In addition to some peaks at 43.47º, 50.76º, and 74.72º arising from the substrate (γ-Fe), only the peaks corresponding to the B1-type structure of TiN and CrN are present. Specifically, TiN exhibits peaks at 36.25º, 42.47º, and 74.72º, while CrN shows peaks at 37.08º, 43.56º, and 63.54º. These peaks correspond to the (111), (200), and (220) orientations, respectively, in that the orientation was preferentially in the (200) direction. Consistent with the findings of other studies, the preferred orientation of CrN layers shifts from the (111) plane to the (200) plane as the bias voltage increases from 20 V to 40 V. In contrast, no shift in the preferred orientation is observed in TiN layers. As the bias voltage increases from 40 V to 60 V, the peak intensity in the (111) and (200) directions decreases, indicating a reduction in the crystallinity of the film.

From a thermodynamic perspective, the shift in preferred orientation aligns with the tendency towards lower energy configurations. This shift can be explained by the mobility of adatoms. At low bias voltages, the mobility of adatoms is low, resulting in the coating being oriented along the (111) plane, which accommodates the highest number of atoms per unit area at low-energy sites. As the substrate bias increases, the mobility of adatoms also increases, promoting the growth of planes with the lowest surface energy, making the (200) texture the preferred orientation [10]. From a kinetic perspective, if coatings are grown under relatively high-ion-energy conditions, their textures tend to evolve towards planes with the most open channels. Consequently, coatings deposited under higher substrate bias change orientation from the (111) plane to the (200) plane, which has more open channeling [15].

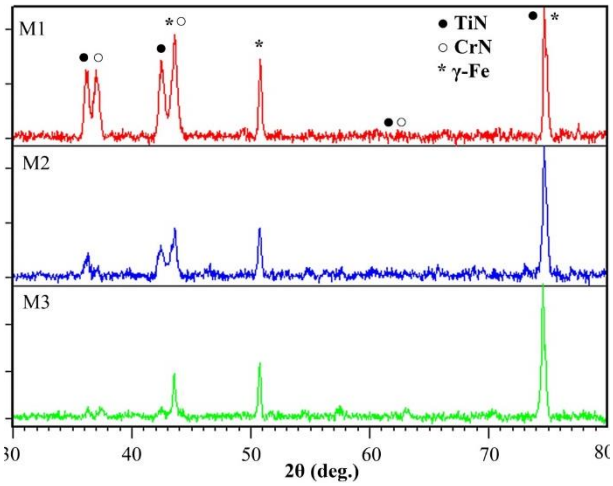

Fig. 1. X-ray diffraction spectra of the coatings.

An increase in bias voltage results in higher ion energy, intensifying the ion bombardment process and subsequently increasing the number of defects in the obtained coating. Consequently, the crystallinity and uniformity of the film diminishes, as evidenced by the reduced intensity of the peaks on the XRD diffraction pattern. In addition, a decrease in crystallinity and uniformity of multilayer coating can be caused by disruption of the development of the TiN columnar structure by the Ti interlayer [16].

The coating surface exhibits defects in the form of pinholes and macroparticles, predominantly spherical in shape (Fig. 2). Additionally, shallow grooves are present on the surface, likely resulting from the sliding of

macroparticles when they come into contact with the rotating sample surface.

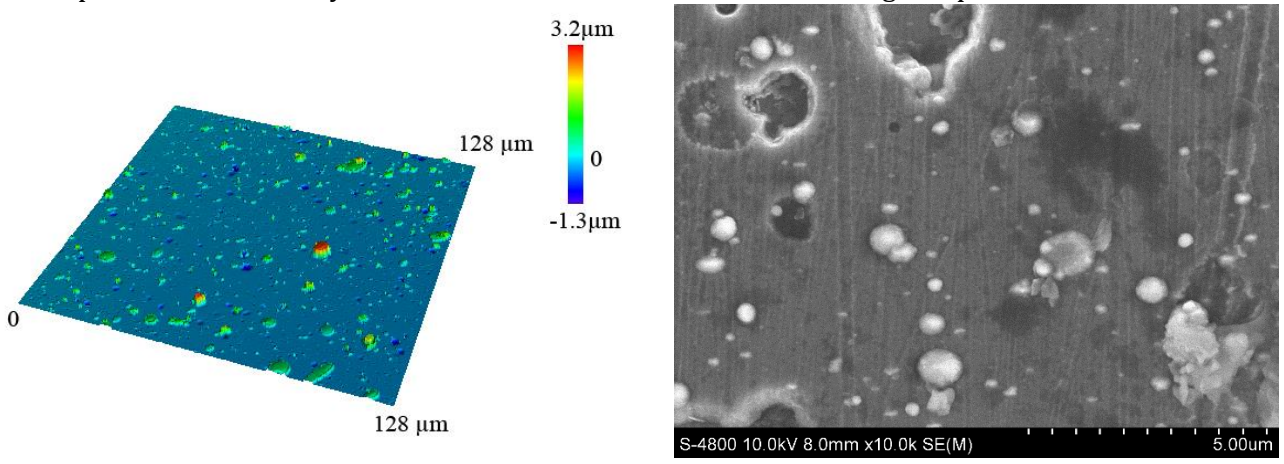

a b

M1

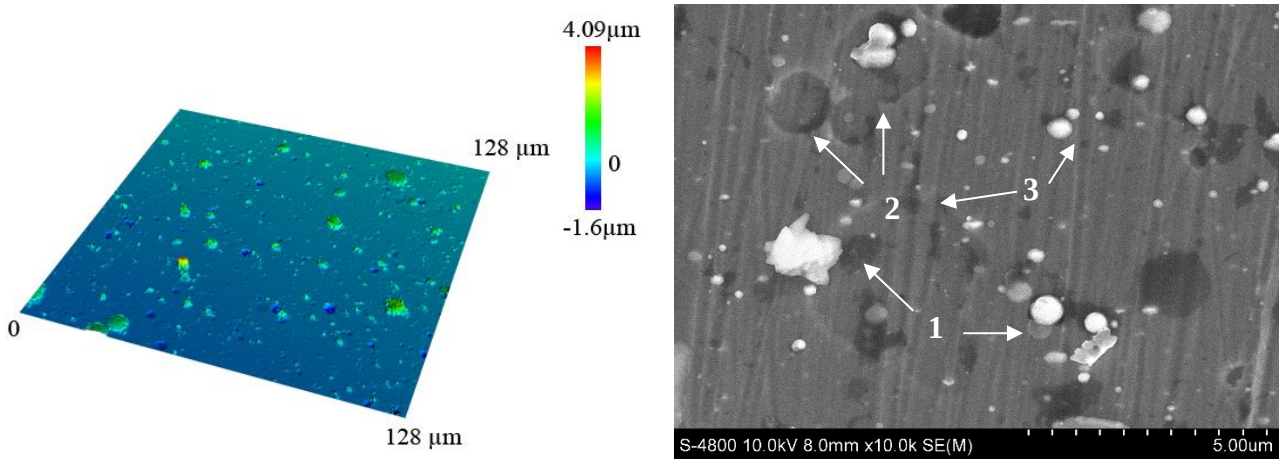

a b

M2

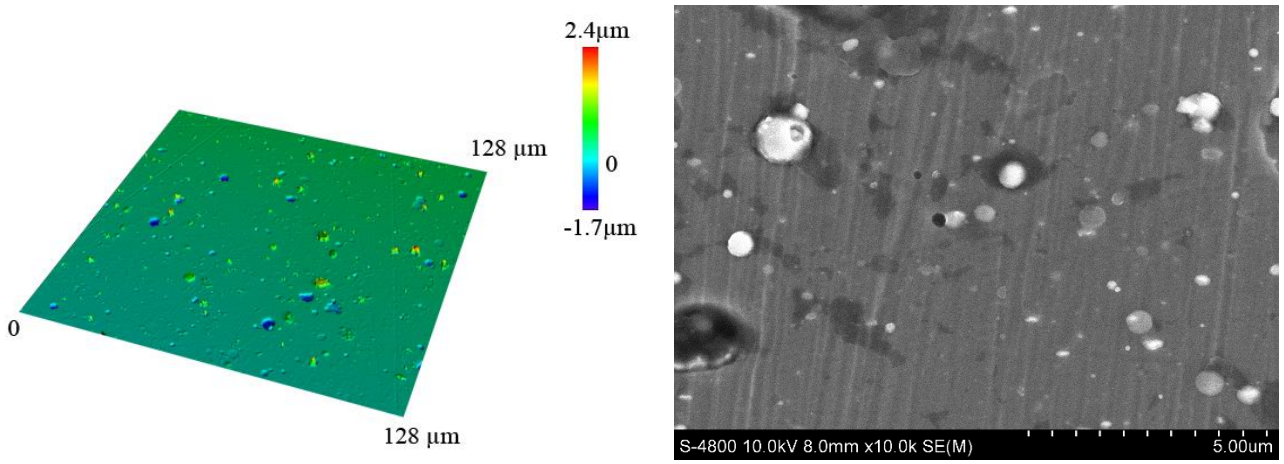

a b

M3

Fig. 2. Sample surface under laser and scanning electron microscope: a) laser images; b) SEM images; 1) Macroparticles; 2) Pinholes; 3) Grooves.

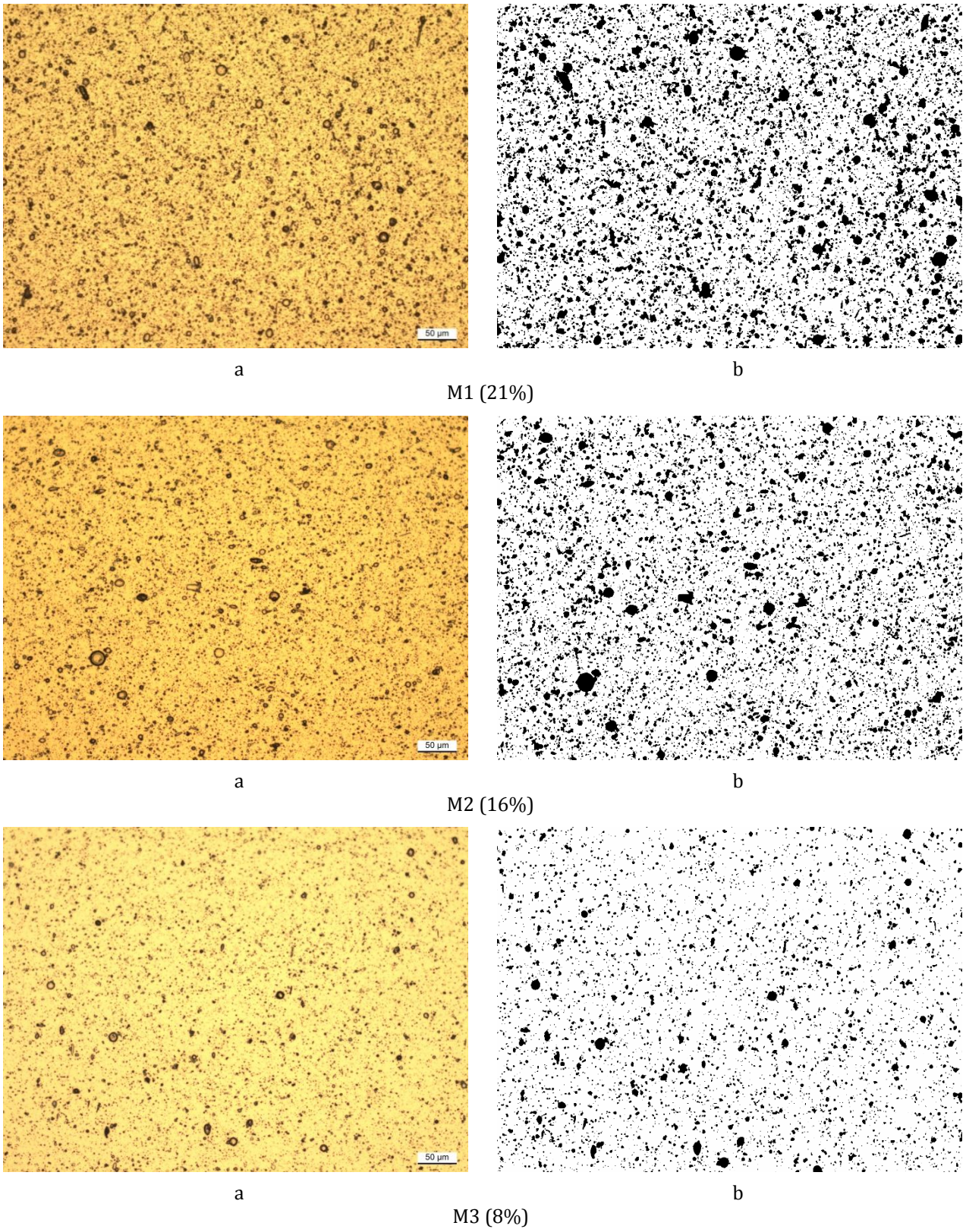

Fig. 3. Sample surface under optical microscope: a) Original images; b) 8 bit image with thresholding for microparticle calculation.

Defect concentration, defined by the percentage of area covered by macroscopic defects such as macroparticles and pinholes, was analyzed. With an increase in bias voltage from 20V to 40V and 60V, a significant decrease in macroscopic defect concentration was

observed, reducing from approximately 21% to 16% and 8%, respectively, as measured from the optical micrographs depicted in Figs. 3. This trend aligns with the findings reported in the study by Valleti et al. [17].

The reduction of defect concentration with increasing substrate bias has been extensively studied and explained in many studies [18-21]. Wang et al. suggest that the main cause of defect reduction is the increase in bias, which leads to a rise in the average energy of the impinging ions. This increase enhances resputtering and diffusion rates, which in turn increases the number of nucleation sites, thereby reducing the number of macroparticles [22]. Studies by Li Zhengyang et al. and Mingsheng Li et al. indicate that applying high bias voltage accelerates the arc plasma through the external electric field. The collisions between incident ions and the coating surface result in the removal of loosely bonded macroparticles. Additionally, before reaching the substrate surface, macroparticles collide with particles in the chamber, such as electrons, ions, or neutral atoms, which alters their charging state to a negative charge. Consequently, the negatively biased substrate exerts a repulsive force on the incoming macroparticles, further reducing their concentration. Additionally, before reaching the substrate surface, macroparticles also collide with particles in the chamber, such as electrons, ions, or neutral atoms, and absorb them. This process makes the marcoparticles negatively charged because the charging effect from electrons is much stronger than that from ions due to the large mass difference between electrons and ions. The negatively biased substrate generates a repulsive force that acts on incoming macroparticles, thereby leading to a reduction in the number of macroparticles [23-24].

Therefore as shown in Fig. 4 the roughness of the films shows a clear tendency to decrease with higher bias voltage during coating deposition. Specifically, as the bias voltage increases from 20 V to 60 V, the average surface roughness (Ra) decreases from 0.227 μm to 0.179 μm, and the average height of macroparticles decreases, as indicated by the reduction in peak height (Rp) from 1.869 μm to 1.489 μm. However, the average depth of the pinholes remains relatively unchanged, ranging from 0.435 μm to 0.439 μm.

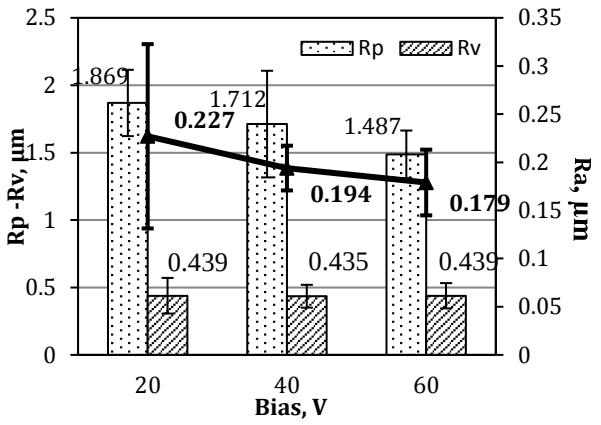

Fig. 4. Relationship between roughness values and the bias voltage.

3.2 Adhesion and thickness

As illustrated in Fig. 5, all samples exhibited an adhesion grade of Class 0, showing no cracks or peeling. This indicates that increasing the substrate bias from 20V to 60V did not affect coating adhesion, as evaluated according to the ISO 26443:2008 standard. Increasing the bias voltage to a certain extent enhances adhesion due to improved coating density. However, significantly increasing the coating thickness under high bias substrate conditions can negatively impact adhesion, as excessive thickness may result in imperfect coatings. Therefore, in practical applications, different negative biases are employed for sublayers during film deposition to ensure necessary adhesion while leveraging the advantages of high bias.

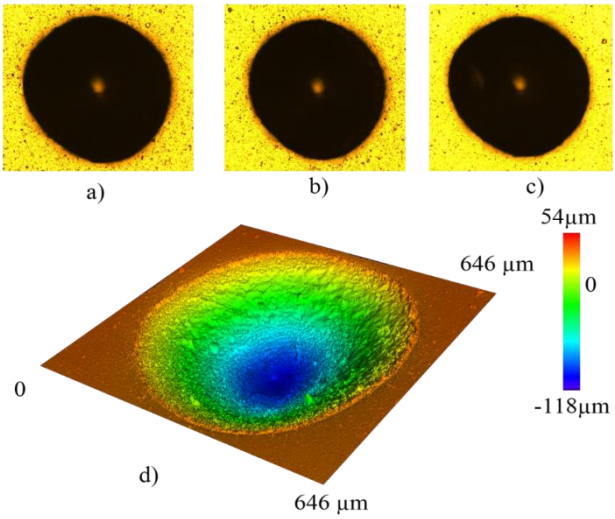

Fig. 5. Sample surface after adhesion test (10x magnification): a) M1; b) M2; c) M3.

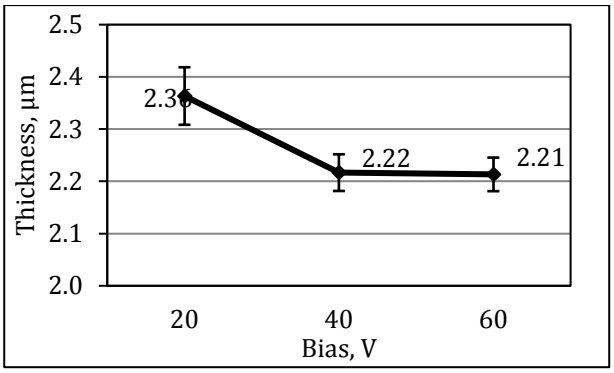

Fig. 6. Coating thickness of studied samples.

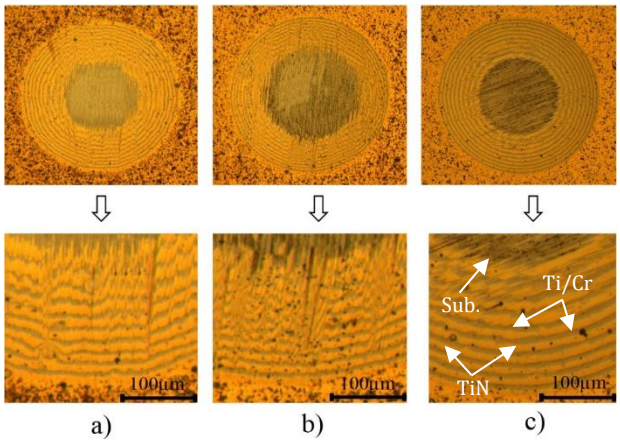

Fig. 7 Thickness measurement coating by Calotest: a) M1; b) M2; c) M3.

The average thickness of Ti/CrN/TiN coatings at different bias voltages is presented in Fig. 6. As the negative bias voltage increases from 20 V to 40 V, the coating thickness decreases sharply from 2.36 µm to 2.22 µm. With further increases in bias voltage up to 60 V, the thickness remains nearly constant, fluctuating between 2.21 µm and 2.22 µm. This decrease in thickness can be attributed to the resputtering of the deposited coating due to energetic ion bombardment as explained above. However, at bias voltages of 40 V and 60 V, the coating thickness stabilizes, likely because the coating density has reached a critical point, requiring additional ion energy to increase further. Fig. 7 shows that calotest measurements reveal alternating light and dark colored circles corresponding to the TiN and Ti/CrN layers, respectively. At higher bias voltages, these circles tend to be smoother due to reduced surface roughness and a lower number of macroparticles. Conversely, at lower bias voltages, the increased number of macroparticles on the surface of each sublayer results in rougher circles.

3.3 Mechanical properties

Fig. 8 presents the average hardness and elastic modulus of the Ti/CrN/TiN coatings at different bias voltages. As the bias voltage increases from 20 V to 60 V, the hardness rises from 8.93 GPa to 14.43 GPa, and the elastic modulus increases from 314.44 GPa to 425.59 GPa. The hardness of the multilayer coatings shows a rapid increase when the bias is raised from 20 V to 40 V, followed by a slight increase as the bias is further increased to 60 V. This increase in hardness can be attributed to a denser microstructure and significant lattice strain, which indicates the presence of compressive stresses that enhance the mechanical resistance of the coating [7].

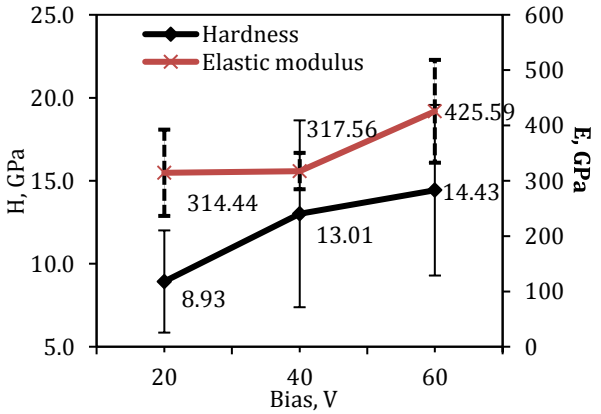

Fig. 8. Dependence of the average hardness and elastic modulus values on bias.

The Ti/CrN/TiN coating exhibits a multilayer structure comprising low-hardness Ti layers alternating with high-hardness CrN/TiN layers. Additionally, macroparticles primarily composed of low-hardness Ti or Cr are present on the surface of the sublayers, causing significant fluctuations in hardness at different penetration depths. As shown in Figure 9, hardness generally tends to decrease with increasing impression depth due to load increase and substrate effect. However, a sudden decrease in hardness can occur when the indenter contacts softer metal such as Ti and Cr.

Increasing the bias voltage to 60 V results in a denser microstructure and significant lattice strain, which suggests the presence of compressive stresses that enhance the mechanical properties of the coating. This phenomenon can be explained by the increased bombardment energy of incident particles on the substrate due to the higher bias voltage. The

enhanced energy causes atoms in the coating to dislodge from their lattice points and move into interstitial positions, leading to a peening effect. Some atoms are directly squeezed between lattice points, causing internal stress and increasing the coating's hardness. However, according to X.S. Wan [25], an excessive increase in bias voltage can reduce hardness due to lattice relaxation and recrystallization, which eliminates crystalline defects.

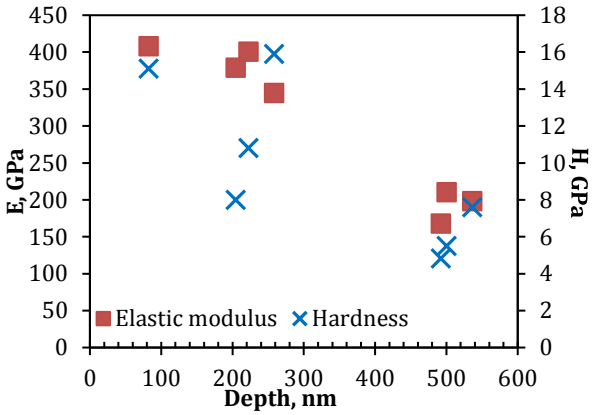

Fig. 9. Dependence of hardness value and average elastic modulus on penetration depths at bias of 20V

3.4 Electrochemical corrosion

The polarization curves and electrochemical properties of the coatings deposited at varying bias voltages are shown in Fig. 10 and Table 2. When the bias is increased from 20 V to 40 V, the corrosion current decreases slightly from 2.29×10^{-07} A to 2.14×10^{-07} A, while the corrosion potential decreases from -0.30501 V to -0.34300 V. Additionally, the corrosion rate decreases from 0.00917 mm/year to 0.001794 mm/year. The polarization curve for the sample coated at a 40 V bias shifts slightly to the left compared to the sample coated at a 20 V bias, with both samples exhibiting a passive region between 0.2 mV and 0.8 mV, where the corrosion current increases slowly as the applied potential increases. Once the applied potential reaches the critical value of 0.8 mV, known as the breakdown potential, the coating's protective ability against corrosion is compromised, resulting in a rapid increase in corrosion current and a vigorous corrosion process.

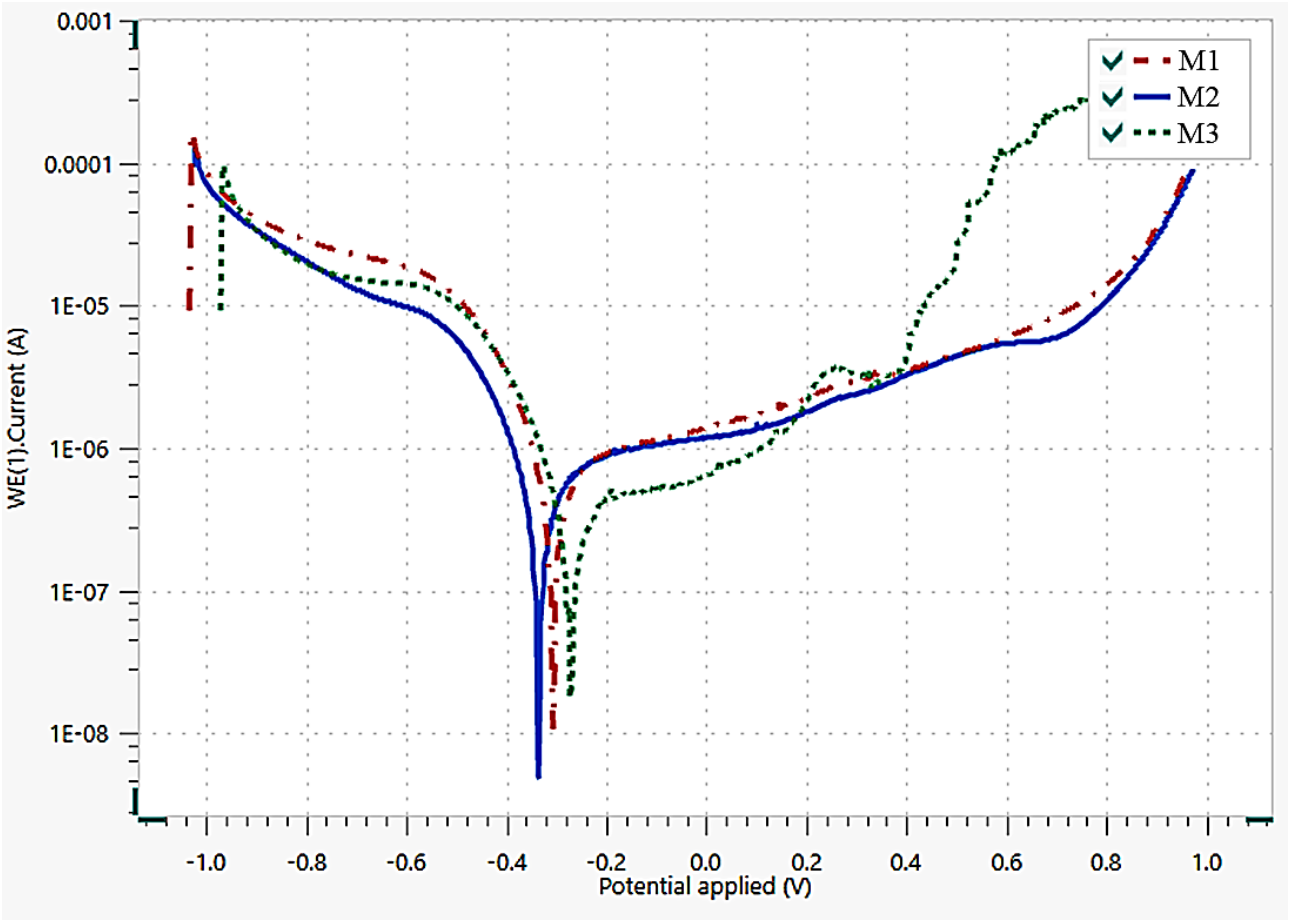

Fig. 10. The potentiodynamic polarization curves of the SUS304 steel coated Ti/CrN/TiN in the 3.5 wt.% NaCl.

Table 2. Electrochemical properties of Ti/CrN/TiN coatings.

Sample	Ecorr, Obs (V)	icorr (A)	Polarization resistance (Ω)	E Begin (V)	E End (V)	Corrosion rate (mm/year)
M1	-0,30501	$2,29\times10^{-07}$	79452	-0.35934	-0.24948	0,001917
M2	-0,34300	$2,14\times10^{-07}$	80800	-0,38818	-0,30029	0,001794
M3	-0,27016	$1,33\times10^{-07}$	133150	-0,31036	-0,23468	0,001113

For the sample coated at a bias of 60 V, the polarization curves exhibit a noticeable shift to the right and downward. The corrosion current decreases to 1.33×10^{-07} A, and the corrosion potential shows a slight positive shift to -0.27016 V, indicating improved corrosion resistance of the films [26]. The corrosion rate is further reduced to 0.001113 mm/year. However, as the applied potential increases, the polarization curves display two small passive regions between -0.2 mV to 0 mV and 0.2 mV to 0.4 mV, as illustrated in Fig. 10, with the breakdown potential decreasing to 0.4 mV.

The favorable corrosion behavior of the coating can be attributed to its dense microstructure and small grain size [20]. Previous studies [21-22] have demonstrated that smaller grain sizes enhance corrosion resistance compared to larger grains. Furthermore, corrosive solutions can more easily penetrate coatings with lower densification. Thus, the coating deposited at 40 V exhibits higher density and, consequently, better corrosion resistance. However, increasing the bias to 60 V results in a lower corrosion rate but narrows the passive region, leading to a faster corrosion process in later stages. This can be explained by the increased defect density in the coating, which diminishes crystallinity and uniformity. Atoms in defect-rich areas have higher free chemical energy compared to those in denser areas, making them more reactive with the corrosive solution and creating corrosion sites on the coating surface. Additionally, cracks and grain boundaries provide preferential channels for corrosive agents to reach the substrate [27].

4. CONCLUSION

The study demonstrates several key findings regarding the impact of bias voltage on Ti/CrN/TiN multilayer coatings. As the bias voltage increases from 20 V to 40 V, the preferred orientation of CrN layers shifts from the (111) plane to the (200) plane, while the TiN layers show no such shift. Further increasing the bias voltage from 40 V to 60 V results in a reduction in film crystallinity, as indicated by the decreased peak intensity in the (111) and (200) directions. All films deposited at 20 V, 40 V, and 60 V comply with the ISO 26443:2008 standard, exhibiting an adhesion grade of Class 0 with no cracks or peeling. The coating surface contains defects such as pinholes and spherical macroparticles. The concentration of these macroscopic defects significantly decreases with an increase in bias voltage, dropping from approximately 21% at 20 V to 16% at 40 V, and 8% at 60 V. Correspondingly, the average surface roughness (Ra) decreases from 0.227 μm to 0.179 μm as the bias voltage increases from 20 V to 60 V. The coating thickness decreases sharply from 2.36 μm to 2.22 μm as the bias voltage increases from 20 V to 40 V, and remains nearly constant between 2.21 μm and 2.22 μm with further increases up to 60 V. The hardness and elastic modulus of the multilayer coating increase from 8.93 GPa and 314.44 GPa at 20 V to 14.43 GPa and 425.59 GPa at 40 V, with minimal changes observed at 60 V. Coatings deposited at a bias of 40 V exhibit favorable electrochemical properties, including a low corrosion rate and a wide passive region from 0.2 mV to 0.8 mV. However, at 60 V, the passive region narrows and corrosion resistance decreases due to the accumulation of defects within the membrane structure.

Acknowledgements

The findings presented herein stem from the results of Project T-1.17 "Development of Technology for Applying High-Durability Protective Coatings Against Corrosion Utilizing Various Materials and Composite Materials Through Ion Beam and Magnetron Sputtering Methods" sponsored by Joint Vietnam-Russia Tropical Science and Technology Research Center. Our heartfelt appreciation extends to the various agencies, institutes, and colleagues whose unwavering support significantly contributed to the successful execution of this project.

REFERENCES

[1] B. Warcholinski, and A. Gilewicz, "Effect of substrate bias voltage on the properties of CrCN and CrN coatings deposited by cathodic arc evaporation," *Vacuum*, vol. 90, pp. 145-150, Apr. 2013, doi: 10.1016/j.vacuum.2012.04.039.

[2] N. S. Mansoor, A. Fattah-alhosseini, H. Elmkhah, and A. Shishehian, "Comparison of the mechanical properties and electrochemical behavior of TiN and CrN single-layer and CrN/TiN multi-layer coatings deposited by PVD method on a dental alloy," *Mater. Res. Express*, vol. 6, no. 12, p. 6, Jan. 2020, doi: 10.1088/2053-1591/ab640d.

[3] E. Lotfi-khojasteh, M. Sahebazamani, H. Elmkhah, M. Nouri, O. Imantalab, and A. Fattah-alhosseini, "A study of the electrochemical and tribological properties of TiN/CrN nano-layer coating deposited on carburized-H13 hot-work steel by Arc-PVD technique," *Journal of Asian Ceramic Societies*, vol. 1, pp. 270-282, Dec. 2020, doi: 10.1080/21870764.2020.1863577.

[4] S. Calderon, C. F. A. Alves, N. K. Manninen, A. Cavaleiro, and S. Carvalho, "Electrochemical corrosion of nano-structured magnetron-sputtered coatings," *Coatings*, vol. 682, no 9 p. 28 Oct. 2019, doi: 10.3390/coatings9100682.

[5] M. Ben Daia, P. Aubert, S. Labdi, C. Sant, F. A. Sadi, Ph. Houdy, and J. L. Bozet, "Nanoindentation investigation of Ti/TiN multilayers films," *Journal of Applied Physics*, vol. 87, pp. 7753-7757, Jun. 2000, doi: 10.1063/1.373450.

[6] C. L. Chang, and C. S. Huang, "Effect of bias voltage on microstructure, mechanical and wear properties of Al–Si–N coatings deposited by cathodic arc evaporation," *Thin Solid Films*, vol. 519, pp. 4923–4927, May 2011, doi: 10.1016/j.tsf.2011.01.054.

[7] M. L. Cedeño, E. A. Diego, M. Juan, G. C. Rodríguez, E. Ovalle, J. González-Hernández, and A. O. Juan, "Effect of Graded Bias Voltage on the Microstructure of arc-PVD CrN Films and its Response in Electrochemical & Mechanical Behavior," *Materials Science (cond-mat.mtrl-sci)*, Oct. 2018, doi: 10.48550/arXiv.1810.07293.

[8] F. Talha, K. Abdullah, A. Rashid, and K. Imran, "Effect of Bias Voltage on Adhesion and Corrosion Resistance of Titanium Nitride Coated Stainless Steel Substrate," *Advanced Materials Research*, vol. 1174, pp. 103-112, Sep. 2022, doi: 10.4028/p-nf315p.

[9] B. Warcholinski, and A. Gilewicz, "Effect of substrate bias voltage on the properties of CrCN and CrN coatings deposited by cathodic arc evaporation," *Vacuum*, vol. 90, pp. 145-150, Apr. 2013, doi: 10.1016/j.vacuum.2012.04.039.

[10] Z. Wang, Z. Dong, K Pei-ling, Li. Xincai, and A. Wang, "Influence of Substrate Negative Bias on Structure and Properties of TiN Coatings Prepared by Hybrid HIPIMS Method," *Journal of Materials Science & Technology*, vol 31, pp. 37-42, Jan. 2015, doi: 10.1016/j.jmst.2014.06.002.

[11] M. Odén, C. Ericsson, G. Håkansson, and H. Ljungcrantz, "Microstructure and mechanical behavior of arc-evaporated Cr–N coatings," *Surface and Coatings Technology*, vol. 114, pp. 39-51, Apr. 1999, doi: 10.1016/S0257-8972(99)00019-5.

[12] K. Chin-Chiuan, L. Yu-Tse , C. Adeline, and C. Jing-Tang. "High Temperature Wear Behavior of Titanium Nitride Coating Deposited Using High Power Impulse Magnetron Sputtering,". *Coatings*, vol. 9, Aug. 2019, doi: 10.3390/coatings9090555.

[13] T. He, Zh. Valery, V. Alexey, C. Vadzim, Y.Huo, M. Filipp Milovich, S. Catherine Sotova, S. Anton and S. Olga. "Comparison of the Mechanical Properties and Corrosion Resistance of the Cr-CrN, Ti-TiN, Zr-ZrN, and Mo-MoN Coatings," *Coatings*, vol. 13(4), Apr. 2023, doi: 10.3390/coatings13040750.

[14] S. Papavinasam, "Electrochemical polarization techniques for corrosion monitoring," *in Elsevier eBooks*, 2021, pp. 45–77. doi: 10.1016/b978-0-08-103003-5.00003-5.

[15] S. Wan-Jui, T. Ming, C. Yee-Shyi, and Y. Jien-Wei, "Effects of substrate bias on the structure and mechanical properties of (Al1.5CrNb0.5Si0.5Ti)Nx coatings," *Thin Solid Films*, vol. 520 ,pp. 6183-6188, Jul. 2012, doi: 10.1016/j.tsf.2012.06.002.

[16] Shanaghi, S. Ghasemi, P. Chu, Sh. Ahangarani, and Y. Zhao, "Effect of Ti interlayer on corrosion behavior of nanostructured Ti/TiN multilayer coating deposited on TiAl6V4," *Materials and Corrosion*, vol. 70, pp. 2113-2127, Jul. 2019, doi: 10.1002/maco.201910883.

[17] K. Valleti, A. Jyothirmayi, M. Ramakrishna, and S.V. Joshi, "Influence of substrate temperature and bias voltage on properties of chromium nitride thin films deposited by cylindrical cathodic arc deposition," *Vacuum Science & Technology A: Vacuum, Surfaces, and Films*, vol. 29, p. 51515, Aug. 2011, doi: 10.1116/1.3625234.

[18] K. Aouadi, B. Tlili, C. Nouveau, A. Besnard, M. Chafra, and R. Souli, "Influence of Substrate Bias Voltage on Corrosion and Wear Behavior of Physical Vapor Deposition CrN Coatings," *Journal of Materials Engineering and Performance*, vol. 28, pp. 2881-2891, Apr. 2019, doi: 10.1007/s11665-019-04033-y.

[19] B. Biswas, Y. Purandare, I. Khan, and P. Hovsepian, "Effect of substrate bias voltage on defect generation and their influence on corrosion and tribological properties of HIPIMS deposited CrN/NbN coatings," *Surface and Coatings Technology*, vol. 344, pp. 383-393, Jun. 2018, doi: 10.1016/j.surfcoat.2018.03.009.

[20] J. Ding, Q.M. Wang, Z. Liu, S. Jeong, Z. Teng Fei, and K. Kwang, "Influence of bias voltage on the microstructure, mechanical and corrosion properties of AlSiN films deposited by HiPIMS technique," *Journal of Alloys and Compounds*, vol. 772, pp. 112-121, Jan. 2019, doi: 10.1016/j.jallcom.2018.09.063.

[21] C. Luo, H. Zhang, J. Shang, and Sh. Duo, "Effect of Bias Voltage on Microstructure and Mechanical Properties of CrN Coatings Prepared by Single Target Magnetron Sputtering," *Key Engineering Materials*, vol. 679, pp. 777-780, Jul. 2016, doi: 10.4028/www.scientific.net/KEM.697.777.

[22] Q.M. Wang, and K. Kim, "Effect of negative bias voltage on CrN films deposited by arc ion plating . II. Film composition, structure, and properties," *Journal of Vacuum Science & Technology A: Vacuum, Surfaces, and Films*, vol. 26, pp. 1267-1276, Aug. 2008, doi: 10.1116/1.2966434.

[23] L. Zhengyang, Z. Wubiao, Z. Yong, L. Guiyingi, and E. Cao, "Effects of superimposed pulse bias on TiN coating in cathodic arc deposition," *Surface and Coatings Technology*, vol. 131, pp. 158-161, Sep. 2000, doi: 10.1016/S0257-8972(00)00754-4.

[24] L. Mingsheng, and F. Wang, "Effects of nitrogen partial pressure and pulse bias voltage on (Ti,AI)N coatings by arc ion plating," *Surface and Coatings Technology*, vol. 167, pp. 197-202, Apr. 2003, doi: 10.1016/S0257-8972(02)00895-2.

[25] X.S. Wan, S.S. Zhao, Y. Yang, J. Gong, and C. Sun, "Effects of Nitrogen Pressure and Pulse Bias Voltage on the Properties of Cr–N Coatings Deposited by Arc Ion Plating," *Surface & Coatings Technology*, vol. 204, pp. 1800-1810, Feb. 2010, doi: 10.1016/j.surfcoat.2009.11.021.

[26] L. Yanhong, J. Li, X. Liu, H. Li, H. Zhou, and J. Chen, "Influence of substrate bias voltage on structure and properties of the CrAlN films deposited by unbalanced magnetron sputtering," *Applied Surface Science*, vol. 258, pp. 3864-3870, Feb. 2012, doi: 10.1016/j.apsusc.2011.12.048.

[27] M. Flores, L. Huerta, R. Escamilla, E. Andrade, and S. Muhl, "Effect of substrate bias voltage on corrosion of TiN/Ti multilayers deposited by magnetron sputtering," *Applied Surface Science*, vol. 253, pp. 7192-7196, Jun. 2007, doi: 10.1016/j.apsusc.2007.02.203.